Multiscale modeling of point defects in Si-Ge(001) quantum wells

B. Yang[1,*] and V. K. Tewary[2]
[1]*Department of Mechanical and Aerospace Engineering, Florida Institute of Technology, Melbourne, Florida 32901, USA*
[2]*Materials Reliability Division, National Institute of Standards and Technology, Boulder, Colorado 80305, USA*
(Received 6 November 2006; published 9 April 2007)

A computationally efficient hybrid Green's function (GF) technique is developed for multiscale modeling of point defects in a trilayer lattice system that links seamlessly the length scales from lattice (subnanometers) to continuum (bulk). The model accounts for the discrete structure of the lattice including nonlinear effects at the atomistic level and full elastic anisotropy at the continuum level. The model is applied to calculate the discrete core structure of point defects (vacancies and substitutional impurities) in Si-Ge(001) quantum wells (QWs) that are of contemporary technological interest. Numerical results are presented for the short range and long range lattice distortions and strains in the lattice caused by the defects and their formation energy and Kanzaki forces that are basic characteristics of the defects. The continuum and the lattice GFs of the material system are used to link the different length scales, which enables us to model the point defects and extended defects such as the quantum well in a unified formalism. Nonlinear effects in the core of the point defects are taken into account by using an iterative scheme. The Tersoff potential is used to set up the lattice structure, compute the unrelaxed forces and force constants in the lattice, and derive the elastic constants required for the continuum GF. It is found that the overall elastic properties of the material and the properties of defects vary considerably when the material is strained from the bulk to the QW state. This change in the defect properties is very significant and can provide a characteristic signature of the defect. For example, in the case of a single vacancy in Ge, the strain reverses the sign of the relaxation volume. It is also found that the defect properties, such as the defect core structures, change abruptly across a Ge/Si interface. The transition occurs over a region extending from two to four lattice constants, depending upon the defect species.

DOI: 10.1103/PhysRevB.75.144103 PACS number(s): 61.72.Bb, 68.65.Fg, 61.72.Ji, 61.82.Fk

I. INTRODUCTION

We describe a hybrid Green's function method for multiscale modeling of point defects such as vacancies and substitutional impurity atoms in a semiconductor lattice containing a quantum well (QW). We apply our model to calculate the core structure of the point defects in the presence of a QW and their strain fields. We also calculate the changes in the interplanar spacing, the lattice constant, and the effective elastic constants of the material caused by the defects. These results should be useful in the design of devices and for study of their mechanical properties. Knowledge of the core structure of defects is also needed for calculation of electronic wave functions in order to model the electronic structure of the defect. In addition, we calculate the Kanzaki force[1] and the formation energy of the defects. These are important parameters for characterization of the defects and can be related to measurable quantities such as relaxation volume, surface stress, and defect diffusion coefficient.[2] Our model includes the nonlinear effects in the core and fully accounts for the elastic anisotropy.

Currently there is a strong technological interest in QWs because of their potential application in the next generation of electronic and photonic devices. In general, point defects are of great importance in the engineering design of electronic materials and devices.[3,4] Point defects are lattice defects and affect mechanical as well as electronic characteristics of devices. They may be desirable or undesirable. For example, point defects are introduced deliberately into lattices to design tailor-made materials with specific properties. They may also emerge naturally when the material is in service. They may act as carrier traps or recombination centers, undermining the performance of the devices. They may coalesce to form major defects such as impurity clusters, cracks and voids that are detrimental to the structural integrity of devices.

The effect of point defects is even more significant in nanostructured devices. This is because the range of interaction between the point defects and extended defects such as surfaces and interfaces is comparable to the dimensions of the device. The electronic and photonic properties of QWs are particularly sensitive to the presence of point defects. A mathematical model is needed to calculate the changes in the mechanical and electronic properties of the material caused by the presence of a QW and the point defects, and also to identify the parameters that can be used to characterize and simulate the defects. Hence it is important to develop robust and reliable techniques for mathematical modeling of point defects in the presence of a QW in a semiconductor.

A semiconductor containing a QW can be visualized as a trilayer material system consisting of a thin layer of a semiconductor sandwiched between two layers of the host. The thickness of a QW is of nanometer order but its lateral dimensions can be macroscopic. Hence it can be regarded as an extended layer defect in the host semiconductor, in contrast to a point defect, which is a zero-dimensional microscopic defect. It is therefore necessary to use a multiscale formulation that can model a point defect as well as a QW in the same formalism in a unified and consistent manner.

The properties of point defects in bulk materials can be calculated by using the continuum model,[5,6] which is reliable only in the far field region. Near field properties or the core structure of a defect in a homogeneous bulk material can be

calculated from first principles or by using a lattice theory based upon an empirical interatomic potential. However, these approaches become computationally very difficult when extended defects such as surfaces, interfaces, or QWs are present in addition to point defects. This is because the problem then involves multiple length scales ranging from subnanometers (interatomic spacing) to nanometers and to continuum (bulk). This is, presumably, the reason why in spite of a vast amount of literature on point defects in bulk materials, no work has been reported on modeling of point defects in QW systems.

Theoretically, first-principles calculations can provide accurate results for the defect core structure.[7,8] However, this class of methods is computationally limited to very small models because of the necessity to include a large number of degrees of freedom in the electronic wave functions. Another approach for modeling a point defect is the molecular dynamics (MD) simulation, in which the atoms are modeled as pointlike particles in an empirical potential field.[9,10] The molecular dynamics (MD) simulation can tackle a much larger system than the first-principles calculations, but is limited because of the necessity to use a small time step, whereas a typical defect process involves much longer time scales.

Green's function method is a powerful technique which is applicable to continuum[5,6] as well as lattice models.[11] The static properties of lattice defects can be efficiently modeled by using the lattice statics Green's function (LSGF).[12] The LSGF is the zero frequency limit of the phonon Green's function.[11] Hence the techniques developed for calculation of the phonon Green's functions,[11] such as the Dyson equation, can be used for the LSGF. In some papers,[13,14] solution of the Dyson equation has been avoided by an elegant use of flexible boundary conditions, but it is not clear *a priori* how much error is introduced by this approximation. In its original form,[12] the LSGF method is limited to localized simple defects in otherwise perfect lattices within the harmonic approximation. Its multiscale version[15] has been used to model a point defect and a free surface. However, this method is not applicable to systems where the point defect is close to the surface and if the nonlinear effects are significant.

Recently, Yang and Tewary[16] have developed a hybrid multiscale LSGF method which is applicable even if the defect is close to the surface. In this approach, the LSGF is calculated numerically for a supercell of atoms under a half-space CGF boundary condition. If the cell is open at the surface, the force-free boundary condition is imposed on the free-boundary atoms instead of the CGF boundary condition. The technique links the multiple scales seamlessly by exploiting the asymptotic approach of LSGF to CGF[12,15] at large distances. This makes it possible to model the point defects at different scales in a unified way by using appropriately dispersed forces, which forms the basis of our multiscale formulation in this paper.

To characterize the mechanical behavior of point defects, two parameters are particularly useful: formation energy and the Kanzaki force. Formation energy of a defect is a well-known parameter. It is defined as the change in the energy of the solid due to the introduction of the defect. It partially determines the defect diffusion coefficient, and is required in a phenomenological simulation of defect diffusion.[2] The Kanzaki force[1] is an equivalent force (system) to the defect to cause the same displacement field in a reference lattice as the defect to cause in the defect lattice. It consists of two terms: (a) a mechanical force, and (b) a force arising due to the lattice relaxation. In the harmonic approximation, part (b) is simply equal to the change in force constants times the associated lattice distortion. Nonlinear effects can also be included in the Kanzaki force. Although the Kanzaki force was introduced about 50 years ago, it is only in the past few years that its usefulness has been recognized[15] for multiscale modeling. It contains all the discrete lattice effects near the defect and, as we show here, it provides a characteristic signature of the defect that can be used to characterize the defect. Both of the above defect parameters, formation energy and the Kanzaki force, can be extracted from the defect core structure.

We also show another very useful property of the Kanzaki force. It can be used to model a defect as an equivalent "inclusion" in the continuum theory. In this approach a defect is treated as an effective inclusion that causes no change in the force constants, but exerts forces only on the atoms of the reference lattice. The effects of the discrete core structure of the defect and the change in the force constants are included in the Kanzaki force. The Kanzaki force can be used to define a series of force and force multipole tensors applied at the defect center position. The moments of the force multipole tensors can be identified with the well-known eigenparameters used in the continuum model. This provides a convenient basis for using the conventional continuum models of lattice defects,[5,6] while still retaining the discrete lattice effects in the core of the defect.

An important input to all the lattice calculations is the interatomic potential. All atomistic defect calculations are based upon minimizing the free enthalpy of the solid that consists of an ionic part which gives the elastic contribution, and an electronic part. These are, of course, coupled. When a defect such as a vacancy is introduced in the lattice, the relaxed configuration depends upon the charge states of the defect.[17] The same applies to extended defects such as a quantum dot or a QW. A rigorous calculation of the relaxed configuration would require an *ab intio* quantum mechanical modeling of the coupled ion-electron system in the whole lattice. Such calculations, as discussed earlier in this section, are limited to very small model crystallites consisting of only a few hundred atoms. At the other extreme is the continuum model, in which the electron effects are totally neglected. The continuum model reproduces the bulk mechanical characteristics of the defect and has been extensively used for a long time. It has the advantage of computational convenience but obviously has a limited validity.

The intermediate approach is to use models in which the effect of the electrons is included in an empirical and phenomenological manner by using an effecting interatomic potential. This approximation has been used in almost all lattice-statics/lattice-dynamics/molecular-dynamics defect calculations, including the present paper. See, for example, the review paper by Stangl *et al.*[18] and the monographs by Harrison[19] and Bimberg *et al.*[20] for application of phenomenological potentials to semiconductors. Such model potentials have been used in many atomistic calculations in Ge/Si

and other semiconductors using molecular dynamics. See, for example, the papers by Makeev and Madhukar,[21] and Swadener *et al.*,[22] which also give other references.

As discussed by Harrison (Ref. 19, Chap. 9), the inherent assumptions in all these calculations are: (i) tight binding approximation which allows us to treat atoms as separate entities, (ii) adiabatic approximation which assumes that the electrons respond adiabatically to the ionic displacements, and (iii) the independent electron approximation. These assumptions result into a separation of the crystal Hamiltonian into a part that gives the relaxation energy of the lattice and another part that gives the energy levels of the electrons. The effect of the electrons on the relaxation energy of the defect is included in an effective model potential. Such models[23–25] give correct values for many observable parameters including the energy of vacancies and other defects, which lends credence to the validity of the model potential. The Tersoff potential[23] that we use in this paper belongs to this class of models. Some other potentials are available in the literature,[18–20] which all have comparable advantages. We have used the Tersoff potential because of its computational convenience in dealing with group IV multi-component systems. It reproduces the correct energy of the defect and has been widely used in defect calculations on covalent solids.

In the present study, we apply our hybrid Green's function (GF) method[16] to study point defects in Si-Ge quantum wells (QWs), a technologically important nanostructure.[19] In Sec. II, the GF method of lattice defects is summarized. Nonlinear effects in the core of a defect are taken into account by using an iterative process, similar to the scheme discussed in previous papers.[26,27] In Sec. III, the reference system of Si-Ge QWs is set up based upon the Tersoff potential of C, Si, and Ge atoms.[23] The Si and Ge lattices retain cubic anisotropy (cubic symmetry with elastic anisotropy) when relaxed, but develop tetragonal anisotropy when strained in their QW states. Then the hybrid GF[16] is calculated using the supercell model under a corresponding CGF boundary condition.[28,29]

In Sec. IV, the core structures of following point defects in Si-Ge QWs are calculated: single vacancy, substitutional C atom, substitutional Si atom in the Ge lattice, and substitutional Ge atom in the Si lattice. The Kanzaki force and the formation energy of these defects are found to differ considerably when the lattice is strained from the relaxed to the QW state. Some components of the Kanzaki force dipole tensor of a single vacancy in Ge matrix are found to switch sign in this course. This is explained by the fact that the atoms surrounding a vacancy are displaced outwards when the lattice is relaxed, but inwards (in lateral directions) when it is strained. This suggests a buckling-type bifurcation in the defect core with the host lattice strain as the parameter. Finally, the defect properties are examined in the strained QW structures. As expected, they vary sharply across a Si/Ge interface. The transition occurs over a distance ranging from two to four lattice constants, depending on the defect species. Conclusions are presented in Sec. V.

II. GREEN'S FUNCTION METHOD FOR MODELING LATTICE DEFECTS

Consider a generally heterogeneous reference lattice system as schematically shown in Fig. 1(a). It is relaxed and

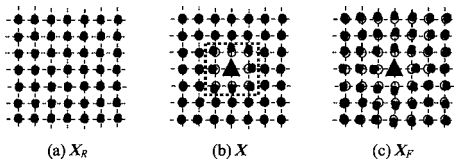

FIG. 1. (a) Reference lattice $\boldsymbol{X}_R$; (b) partially relaxed defect lattice $\boldsymbol{X}$; (c) fully relaxed defect lattice $\boldsymbol{X}_F$. The solid circles represent atoms while the open ones represent the reference lattice sites. The solid triangle represents an impurity atom or a vacancy. In (b), the dotted line defines a nominal nonlinear core in which the atomic position is constantly updated in the iterative solution process.

may contain different species of atoms. The corresponding configuration is indicated by $\boldsymbol{X}_R$, and a defect lattice system is created by introducing point defects such as vacancies, substitutional impurity atoms, and interstitials to the reference system. Our aim is to solve for the fully relaxed configuration $\boldsymbol{X}_F$ of the defect system, as shown in Fig. 1(c). An intermediate (partially relaxed) defect lattice, $\boldsymbol{X}$, is introduced, as shown in Fig. 1(b). This is necessary in order to take into account nonlinear effects in an iterative scheme. The lattice theory[11,12] is summarized below.

Within the theory of lattice statics, the equilibrium of a defect system requires that the interatomic potential energy V is minimized as given by

$$\delta V(\mathbf{x}) = 0. \tag{1}$$

One may expand the potential around the partially relaxed configuration $\boldsymbol{X}$ of the defect system in Fig. 1(b) in the Taylor series as

$$V(\mathbf{x}) = V(\mathbf{X}) + \left(\frac{\partial V}{\partial x_i^{(a)}}\right)_{\mathbf{X}} u_i^{(a)} + \frac{1}{2}\left(\frac{\partial^2 V}{\partial x_i^{(a)} \partial x_j^{(b)}}\right)_{\mathbf{X}} u_i^{(a)} u_j^{(b)} + o(u_i^{(a)} u_j^{(b)} u_k^{(c)}), \tag{2}$$

where the subscripts indicate components of a tensor, the superscripts indicate the attachment to a certain atom, $\boldsymbol{u}$ is the atomic displacement, defined by $\mathbf{u}=\mathbf{x}-\mathbf{X}$, and repeated subscripts (and superscripts) imply the conventional summation over their range. Approximating the potential up to the quadratic term and substituting it into Eq. (1) yields

$$\phi_{ij}^{(ab)} u_j^{(b)} = f_i^{(a)}, \tag{3}$$

where the force $\boldsymbol{f}$ and force constants $\boldsymbol{\phi}$ are defined by

$$f_i^{(a)} \equiv -\left(\frac{\partial V}{\partial x_i^{(a)}}\right)_{\mathbf{X}} \text{ and } \phi_{ij}^{(ab)} \equiv \left(\frac{\partial^2 V}{\partial x_i^{(a)} \partial x_j^{(b)}}\right)_{\mathbf{X}}. \tag{4}$$

A solution for the atomic displacement field $\boldsymbol{u}$ of the defect system measured from $\boldsymbol{X}$ can be obtained by inverting the force-constant matrix $\boldsymbol{\phi}$ as

$$u_j^{(b)} = [\phi_{ij}^{(ab)}]^{-1} f_i^{(a)}. \tag{5}$$

Defining $L_{ji}^{(ba)} \equiv [\phi_{ij}^{(ab)}]^{-1}$, the above equation is rewritten as

$$u_j^{(b)} = L_{ji}^{(ba)} f_i^{(a)}. \tag{6}$$

$L_{ji}^{(ba)}$ is the ith displacement component of the a atom caused by a unit point force applied along the jth direction on the b atom, i.e., the *defect* LSGF of the partially relaxed defect system $\boldsymbol{X}$ in Fig. 1(b). Due to the reciprocal theorem, $L_{ji}^{(ba)} = L_{ij}^{(ab)}$.

In order to find the defect LSGF $L_{ji}^{(ba)}$, the force-constant matrix $\boldsymbol{\phi}$ of the partially relaxed defect system is partitioned as

$$\phi_{ij}^{(ab)} = \phi_{ij}^{0(ab)} - \Delta\phi_{ij}^{(ab)}, \tag{7}$$

where $\boldsymbol{\phi}^0$ is the force-constant matrix of the reference system $\boldsymbol{X}_R$ in Fig. 1(a), and $\Delta\boldsymbol{\phi}$ is the difference in the force-constant matrix between the reference system $\boldsymbol{X}_R$ and the partially relaxed defect system $\boldsymbol{X}$. Inverting and rearranging the matrices in Eq. (7) yields

$$L_{ji}^{(ba)} = L_{ji}^{0(ba)} + L_{jk}^{(bc)} \Delta\phi_{kl}^{(cd)} L_{li}^{0(da)}, \tag{8a}$$

and, alternatively

$$L_{ji}^{(ba)} = L_{ji}^{0(ba)} + L_{jk}^{0(bc)} \Delta\phi_{kl}^{(cd)} L_{li}^{(da)}, \tag{8b}$$

where $\mathbf{L}^0 (\equiv [\boldsymbol{\phi}]^{-1})$ is the *reference* LSGF of the reference system. Equation (8) is called the Dyson equation, which relates the LSGFs of the defect and reference lattices through the change in the force-constant matrix $\Delta\phi_{kl}^{(cd)}$. Given $L_{ji}^{0(ba)}$, Eq. (8) can be solved to derive the defect LSGF $L_{ji}^{(ba)}$ and consequently the atomic displacement $u_j^{(b)}$.

Multiplying by force $\boldsymbol{f}$ on both sides of Eq. (8b) and applying Eq. (6) results in

$$u_j^{(b)} = L_{ji}^{0(ba)} f_i^{(a)} + L_{jk}^{0(bc)} \Delta\phi_{kl}^{(cd)} u_l^{(d)}. \tag{9}$$

This is also called the Dyson equation, for the partially relaxed defect lattice $\boldsymbol{X}$ with a specified force system. Given $\boldsymbol{L}^0$, it may be solved for $\boldsymbol{u}$ within the defect space defined by nontrivial $\Delta\boldsymbol{\phi}$. Then, $\boldsymbol{u}$ can be calculated for any atom. Equation (9) may be rewritten as

$$u_j^{(b)} = L_{ji}^{0(ba)} K_i^{(a)}, \tag{10}$$

with

$$K_i^{(a)} = f_i^{(a)} + \Delta\phi_{il}^{(ad)} u_l^{(d)}. \tag{11}$$

The effective force $\boldsymbol{K}$ defined by Eq. (11) is called the Kanzaki force.[1] It models the defect as an inclusion that introduces no change in the interatomic force constants of the reference system $\boldsymbol{X}_R$. This is analogous to the Mura terminology of inclusion modeling a continuum defect as a volume of eigenstrain but introducing no changes in elastic constants to the host material.[5] Note that Eq. (10) is exactly equivalent to Eq. (6).

Recall that the above formulation stems from the truncated Taylor series expansion of the interatomic potential at the quadratic term in Eq. (2). If the higher-order terms are included in Eq. (2), $\boldsymbol{X}$ of Fig. 1(b) plus $\boldsymbol{u}$ obtained from Eq. (10) would not precisely lead to $\boldsymbol{X}_F$ of Fig. 1(c). In such a case, an iterative process is necessary to accurately solve for $\boldsymbol{X}_F$. The following iterative scheme is adopted in the present study.

Based on the previous step, $\boldsymbol{X}$ is updated to $\boldsymbol{X}+\boldsymbol{u}$. With the updated $\boldsymbol{X}$, $\boldsymbol{f}$ and $\boldsymbol{\phi}$ are recalculated by Eq. (4) and inserted into Eq. (9). Then, Eq. (9) is solved for $\boldsymbol{u}$ (measured from the current $\boldsymbol{X}$) within the defect space. Equation (10) is then used to compute $\boldsymbol{u}$ at any atom. Repeating the process until $\boldsymbol{X}+\boldsymbol{u}$ converges leads to the fully relaxed configuration $\boldsymbol{X}_F$, which is the final solution. It should be noted that the above iteration scheme, namely, the classical Newton-Raphson method, would converge only if the force-constant matrix is positive definite in every iteration step. Since it works well in our later simulations, no other nonlinear solvers, such as a modified Newton-Raphson method used in a previous anharmonic lattice GF study,[30] are checked in this study. One may refer to Refs. 31 and 32 among many other textbooks for a detailed discussion of those nonlinear solution methods.

The fully relaxed configuration $\boldsymbol{X}_F$ of a given defect is well defined and unique. In contrast, the Kanzaki force system $\boldsymbol{K}$ is nonunique. By the definition given in Eq. (11), it is distributed over a partially relaxed configuration $\boldsymbol{X}$ in the last step of iteration. This $\boldsymbol{X}$ in turn depends on how the nonlinear defect core is specified, and this specification may be subjective. For the sake of computational efficiency, it is desired only to update $\boldsymbol{X}$ of those atoms involved in appreciable nonlinear deformation in the vicinity of a point defect. Since nothing is clear about the nonlinear zone prior to solution, an arbitrary defect core size would be specified, as shown schematically by the dotted line in Fig. 1(b). In the course of iterative solution, the mechanical forces and displacements measured on the basis of $\boldsymbol{X}$ are both expected to diminish inside the nonlinear core. Thus, the Kanzaki force, as defined in the last iteration step, would appear only around the boundary of the nonlinear defect core. In our case of using the Tersoff potential with interatomic interaction up to the second-nearest neighbors, the number of shells of atoms on which the Kanzaki force may appear is two, if no nonlinear core is specified; three, if a nonlinear core size of one shell of atoms is specified; and four, if a nonlinear core size of more than one shell of atoms is specified. In any case, the Kanzaki force system must appear on two shells of atoms immediately outside the nonlinear core. Although the Kanzaki force system depends on how the nonlinear defect core is specified, the net force and multipole tensors derived from the Kanzaki forces (defined below) must converge with the (nominal) core size and be unique.

The net Kanzaki force (defined as the sum of individual Kanzaki forces) is trivial if the defect is self-balanced. In this case, the force dipole tensor is used to measure the defect intensity, and may represent the defect as viewed at a large distance. It is defined by

$$M_{ij} = (X_i^{(a)} - X_i^{(ave)}) K_j^{(a)}, \tag{12}$$

where $\boldsymbol{X}^{(ave)}$ is the average center position of the defect. Meanwhile, the defect formation energy V_f is defined as the difference in potential energy between the reference system $\boldsymbol{X}_R$ and the fully relaxed defect system $\boldsymbol{X}_F$,

$$V_f = V(\boldsymbol{X}_F) - V(\boldsymbol{X}_R). \tag{13}$$

The above equation, which involves the entire lattice system, is impractical for numerical evaluation. Instead, the formation energy V_f is evaluated by

$$V_f = V(\boldsymbol{X}) + E - W - V(\boldsymbol{X}_R), \tag{14}$$

where $\boldsymbol{X}$ is required to be sufficiently close to $\boldsymbol{X}_F$, and $V(\boldsymbol{X}_R)$ and $V(\boldsymbol{X})$ are the potential energies of the reference and partially relaxed defect lattices $\boldsymbol{X}_R$ and $\boldsymbol{X}$. E is the harmonic deformation energy and W is the work (i.e., relaxation energy), given by

$$E = \frac{1}{2}\phi_{ij}^{(ab)} u_i^{(a)} u_j^{(b)} \text{ and } W = f_i^{(a)} u_i^{(a)}, \tag{15}$$

where $\boldsymbol{\phi}$ and $\boldsymbol{f}$ are associated with $\boldsymbol{X}$ as defined in Eq. (4), and $\boldsymbol{u} = \boldsymbol{X}_F - \boldsymbol{X}$. To satisfy the above requirement of $\boldsymbol{X}$ being sufficiently close to $\boldsymbol{X}_F$, it is taken to be the configuration at the last step of the iterative solution as described before. Since E is one half of W by virtue of Eq. (3), the formation energy is finally derived as

$$V_f = V(\boldsymbol{X}) - \frac{1}{2} f_i^{(a)} u_i^{(a)} - V(\boldsymbol{X}_R). \tag{16}$$

Equation (16) is convenient and efficient for numerical evaluation as compared to Eq. (13) because it involves only the defect space rather than the entire lattice system.

In brief, an iterative LSGF method has been described in this section to calculate the lattice distortion due to a defect by solving the Dyson equation. The method accounts for the nonlinear effects. The remaining problem is how to find the reference LSGF, $\boldsymbol{L}^0$, used as the summation kernel in the Dyson equation. If the reference system is a perfect (i.e., infinite and homogeneous) lattice, $\boldsymbol{L}^0$ can be efficiently obtained by solving the lattice-statics problem of a very large cell of atoms under a periodic or fixed boundary condition, for instance, by the Fourier transform technique.[12] It can take advantage of the group symmetries, especially the full translational symmetry, of a perfect lattice. However, in the present case of Si-Ge QWs, the reference system is heterogeneous, which lacks the full translational symmetry. Hence, the above technique, which works well in the case of a perfect lattice, does not work here. This difficulty can be overcome by applying the recently developed scheme of hybrid GF,[16] where the reference LSGF is obtained to a desired degree of approximation by solving the lattice-statics problem of a cell of atoms subjected to a unit point force and under a CGF boundary condition. If the LSGF quickly approaches the CGF, the cell size required for accurate evaluation would be fairly small compared to that required in the other techniques. The scheme of hybrid GF for Si-Ge QWs is described in the next section.

III. HYBRID GREEN'S FUNCTION OF Si/Ge(001) QUANTUM WELLS

A. Reference lattice setup and continuum properties

Si-Ge QWs are trilayer material systems consisting of a thin layer of either Si or Ge sandwiched by two opposite half-space substrates of the other, as schematically shown in Fig. 2. The whole diamondlike lattice is assumed to be orientated with the crystallographic axis (001) normal to the interfaces. The thin layer is strained laterally to match the lattice constant with the substrates. It is stretched if the midlayer is Si, and compressed if it is Ge because the lattice constant of Si lattice is smaller than that of the Ge lattice. The entire system is then relaxed. This nanostructure, with layer thickness ranging from several to several tens of nanometers, has been extensively studied and is under technological development.[19]

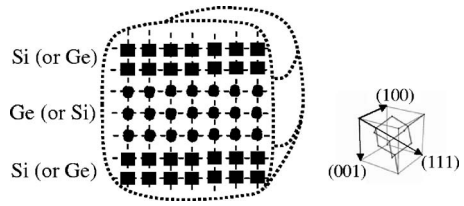

FIG. 2. Schematic of a trilayer reference lattice of a Si/Ge/Si or Ge/Si/Ge QW. Also shown is a unit cell of the diamond lattice structure.

By using the Tersoff empirical potential,[23] the lattice constants are found to be 5.4320 Å and 5.6567 Å in all three base axes in the relaxed Si and Ge, respectively, which remain cubic. When Si is stretched to a lattice constant of 5.6567 Å in the lateral directions, its lattice constant in the third direction is reduced to 5.1952 Å upon relaxation in the same direction. Similarly, when Ge is compressed to a lattice constant of 5.4320 Å in the lateral directions, its lattice constant in the third direction is increased to 5.8145 Å upon relaxation in the same direction. In both the cases the symmetry is reduced from cubic to tetragonal.

The above values of the lattice constants were obtained by inspection of the variation of the potential energy with atomic spacing in the third direction under the condition of fixed lateral dimensions. They correspond to the states of potential minimum under the constraints. Next, these materials are assembled to form desired QWs. The assembled trilayer material systems are relaxed to obtain the correct atomic spacing near the abrupt Si/Ge interface. This is carried out with a sufficiently long column of atoms along the layer-thickness direction, with a cross-section of one unit cell by one unit cell, by utilizing the lateral periodicity of the lattice.

The variation of relaxed atomic interplanar (sheet-to-sheet) spacing for the Si/Ge/Si and the Ge/Si/Ge QWs is given in Tables I and II, respectively. It is shown that the atomic interplanar distance between interfacial Si and Ge atoms is approximately equal to the average of atomic interplanar distance of these two planes of atoms remote from the interfaces. Otherwise, it is altered only slightly near the interfaces. Although the alteration is slight, it is necessary to take it into account in order to establish a force-free reference lattice in equilibrium so that a defect introduced in the lattice can be modeled accurately.

After finding the lattice constants, the elastic properties of the relaxed and strained bulk Si and Ge matrices are examined. The stress in the crystals is defined by

TABLE I. Variation of interplanar atomic spacing with number of interplanar gaps counted about an interface in a Si/Ge/Si QW.

Number of gaps (elements)	−3 (Ge/Ge)	−2 (Ge/Ge)	−1 (Ge/Ge)	0 (Ge/Si interface)	1 (Si/Si)	2 (Si/Si)	3 (Si/Si)
Spacing (Å)	1.4536	1.4533	1.4580	1.4074	1.3542	1.3583	1.3580

$$\sigma_{ij} = \frac{\partial V}{\partial \varepsilon_{ij}}, \tag{17}$$

where ε_{ij} is the infinitesimal strain, defined by

$$\varepsilon_{ij} = \tfrac{1}{2}(u_{i,j} + u_{j,i}). \tag{18}$$

Equation (17) is convenient for evaluation of stress in a relaxed lattice that is subjected to no (body) force. We calculate the "stress" at an atom using the following procedure:

To begin with, the lattice is relaxed and all the neighboring atoms directly interacting with the atom are identified. Then, the neighboring atoms are perturbed by imposing a displacement field according to a specified infinitesimal strain [in the finite-difference form of Eq. (18)]. Finally, the potential energies are calculated at the central atom surrounded by the relaxed and perturbed neighboring atoms, respectively. The difference between the potential energies is set equal to the product of the stress and the perturbing strain tensors. Repeating the above process six times with different perturbing strains, we obtain six such equations, which we solve for the six components of the symmetric stress tensor. For computational convenience, we can assume that at any one time only one component of the perturbing strain is nonzero. Since the stress is essentially a continuum parameter, there is some subjectivity in defining the stress in a discrete lattice model. Different definitions of stress have been proposed[33] for the discrete lattices. The numerical difference between the values of the stress, calculated according to alternative definitions, is small in the static case. Our method of calculating the stress would lead to the exact continuum result[34] with appropriate symmetry in the continuum limit.

The elastic constants of a material element are defined by

$$C_{ijkl} = \frac{\partial \sigma_{ij}}{\partial \varepsilon_{kl}}. \tag{19}$$

Each constant is evaluated numerically by first drawing a sufficiently large cell of atoms, for instance, a block of $20 \times 20 \times 20$ unit cells. A displacement field is then imposed on the atoms according to the strain field specified above. The system is relaxed while the boundary atoms are tightly held. The physical cell boundary consists of two layers of atoms due to the direct interaction of atoms up to the second nearest neighbors in the Tersoff potential used. Finally, the stress at the central atom is calculated as above. The change of stress is set equal to the product of the elastic constants and perturbing strain, resulting in six independent equations. Repeating the above process six times with different perturbing strains, we obtain 6×6 such equations which we solve for all 6×6 components of the elastic stiffness matrix (in the Voigt contracted notation[35]). The elastic stiffness matrix would preserve the full symmetry.

The relaxed bulk Si and Ge are found to retain the cubic anisotropy. The elastic constants in the Voigt contracted notation are: $C_{11}=0.890$, $C_{12}=0.471$, $C_{44}=0.432$ for Si, and $C_{11}=0.865$, $C_{12}=0.277$, $C_{44}=0.417$ for Ge in units of eV/(Å)^3. When Si and Ge are strained in their QW states, they develop tetragonal anisotropy. The corresponding elastic constants in units of eV/(Å)^3 are given by $C_{11}=0.867$, $C_{12}=0.381$, $C_{13}=0.404$, $C_{33}=0.700$, $C_{44}=0.387$, $C_{66}=0.464$ for Si, and by $C_{11}=0.899$, $C_{12}=0.405$, $C_{13}=0.368$, $C_{33}=0.981$, $C_{44}=0.462$, $C_{66}=0.337$ for Ge. It should be noted that in our previous work,[16] the stress was evaluated by averaging the forces transmitted through the boundary of a subcell, and somewhat different elastic constants were obtained. The above results of the relaxed bulk Si are in full agreement with those previously reported in the literature.[34]

B. Hybrid lattice and continuum Green's function

We now derive the hybrid GF by combining the LSGF and the CGF. We apply a unit point force at an atom A in the reference lattice system, as defined in Sec. II, along one of the axes, for instance, the Ith axis. The response to the force is termed the reference LSGF, which must be unique for the reference system subjected to a remote radiation condition, i.e., diminishing displacement at infinity. The system may also be modeled as a trilayer continuum subjected to a unit point force and subjected to the same remote radiation condition. This response is termed the reference CGF. The above two alternative models of the same physical system are linked in the long-wavelength limit, which leads to well known linear relations between the elastic constants and the force constants.[11,36,37]

The force constants, a second-rank tensor, characterize the interaction between two atoms. The elastic constants, a

TABLE II. Variation of interplanar atomic spacing with number of interplanar gaps counted about an interface in a Ge/Si/Ge QW.

Number of gaps (elements)	−3 (Ge/Ge)	−2 (Ge/Ge)	−1 (Ge/Ge)	0 (Ge/Si interface)	1 (Si/Si)	2 (Si/Si)	3 (Si/Si)
Spacing (Å)	1.4142	1.4139	1.4185	1.3616	1.2947	1.2990	1.2988

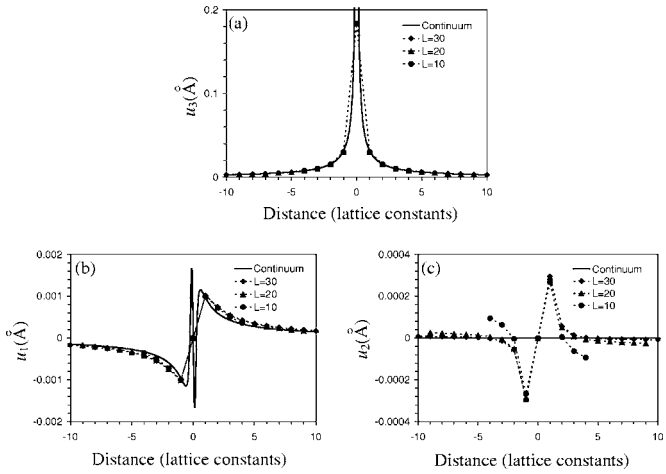

FIG. 3. Variation of displacement components along the (100) direction with distance to a unit point force applied in the (001) direction, normal to the interface. The line of data acquisition passes through the atom where the point force is applied.

fourth-rank tensor, characterize the local behavior of an infinitesimal volume element of the material (assuming local elasticity). It is well known that the LSGF asymptotically approaches the CGF with increasing distance from the force. Therefore, the LSGF may be replaced by the CGF at a sufficiently distant field point. At smaller distances, the LSGF may be calculated under a CGF boundary condition.

We then draw a supercell of atoms around the unit point force. It may be heterogeneous, containing both Si and Ge atoms, if the point force is located near an interface. Layers of atoms that directly interact with any atom outside the supercell are identified as boundary atoms. As mentioned earlier, if the distance between the boundary atoms and the point where the force is applied is sufficiently large, the boundary atoms can be assigned a displacement as given[28,29] by the corresponding trilayer CGF. This reduces the equilibrium equation (3) to the following:

$$\phi_{ij}^{(ab)} u_j^{(b)} = \delta_{Ii}^{(Aa)}, \tag{20}$$

with $a \in$ supercell minus the boundary atoms, and $b \in$ supercell. In Eq. (20) $\delta_{Ii}^{(Aa)}$ denotes the Dirac δ function, which is equal to one if $a=A$ and $i=I$, and zero otherwise. After substituting the CGF for the displacement at the boundary atoms, Eq. (20) can be solved for the displacement of the interior atoms. The solution offers an approximate evaluation of the LSGF, namely, a hybrid GF. It is termed hybrid because it is a combination of the LSGF and CGF, and depends on the size of the supercell.

For illustration, we examine the dependence of hybrid GF on the supercell size in the case of Si/Ge/Si QW with well thickness equal to ten lattice constants. This will also show some of the characteristic features of the trilayer LSGF and CGF. A point force of magnitude equal to one unit (eV/Å) is applied at an interfacial Ge atom in the (001) direction, normal to the interfaces. The induced displacement is calculated along a horizontal line in the (100) direction, passing through the source atom. In the calculation of the CGF, we assume a

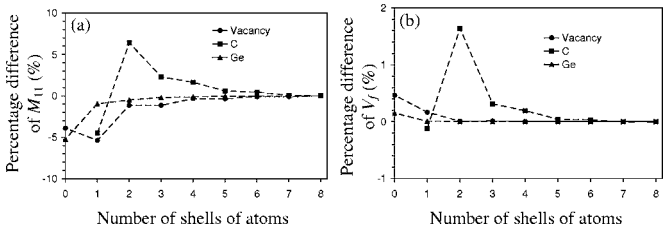

FIG. 4. Percentage variation of (a) Kanzaki force dipole tensor ($M_{11}=M_{22}=M_{33}$) and (b) formation energy V_f obtained with various nonlinear core sizes relative to the results obtained with the largest nonlinear core size of eight shells of neighboring atoms for vacancy, C substitution and Ge substitution in the relaxed bulk Si matrix.

continuum interface of zero thickness at the middle plane between the adjacent Si and Ge sheets. The elastic constants across the interface are discontinuous.

The results with supercell sizes, $L=10$, 20, and 30 lattice constants (in each direction), are plotted in Fig. 3. It is seen that the hybrid GF converges with increasing supercell size. The converged hybrid GF, which is the true LSGF, is generally different from the CGF in the vicinity of the point force, but approaches the CGF at greater distances from the point force. This confirms the asymptotic approach of LSGF to CGF, which is the basis for the present hybrid GF technique.

As we see in Fig. 3, the dominant component u_3, which is in the same direction as the point force, i.e., $L_{33}^{(Ab)}$, becomes equal to its continuum counterpart at a fairly small distance from the point force, that is, at approximately one lattice constant. The difference, of course, is huge close to the point force because the LSGF is finite at zero separation but the CGF is infinite. The other two components of LSGF reduce to their continuum counterparts at a relatively large distance from the point force. They represent some subtle features of the lattice distortion in the diamondlike crystal, especially near the abrupt interface. The value of u_2 as predicted by the lattice model is finite, whereas the continuum solution of u_2 is zero. The continuum solution of u_1 exhibits a near-singular behavior. This is obviously an artifact of the continuum model arising from the assumption of a discontinuous interface of zero thickness.

Note that, although the components u_1 and u_2 approach the CGF at a relatively large distance from the force, they are a few orders of magnitude smaller than the dominant com-

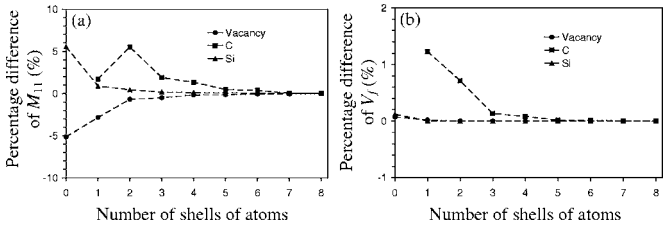

FIG. 5. Percentage variation of (a) Kanzaki force dipole tensor ($M_{11}=M_{22}=M_{33}$) and (b) formation energy obtained with various nonlinear core sizes relative to the results obtained with the largest nonlinear core size of eight shells of neighboring atoms for vacancy, C substitution and Ge substitution in the relaxed bulk Ge matrix.

TABLE III. Kanzaki force dipole tensor and formation energy of point defects in the relaxed and strained Si matrices. The strained case corresponds to the QW state.

	Vacancy		C substitution		Ge substitution	
	Uns. mtrx.	Str. mtrx.	Uns. mtrx	Str. mtrx	Uns. mtrx	Str. mtrx
M_{11} (eV)	5.37	8.22	−16.2	−15.3	1.45	1.32
M_{22} (eV)	5.37	8.22	−16.2	−15.3	1.45	1.32
M_{33} (eV)	5.37	5.31	−16.2	−13.7	1.45	1.52
V_f (eV)	3.70	3.41	−1.63	−1.03	0.806	0.761

ponent u_3. If the point force is away from the interface, for instance, in the middle of the layer, the components u_1 and u_2 are even smaller compared with the dominant component u_3. Therefore, a fairly small supercell can be used for efficient and accurate evaluation of the LSGF, which in turn facilitates an efficient and accurate solution to Eqs. (8) and (9) for modeling of the point defects.

IV. ANALYSIS OF THE POINT DEFECTS

In this section, the above GF method is applied to obtain the nonlinear core structure of various point defects in Si-Ge QWs. Point defects that we consider are: single vacancy, substitutional C atom, substitutional Si atom in the Ge lattice, and substitutional Ge atom in the Si lattice. We show that our hybrid GF technique, combining LSGF and CGF through their asymptotic relationship, facilitates an efficient and accurate solution of the complicated problem of a trilayer system containing point and extended defects at multiple length scales.

As discussed earlier, the nonlinear core size of a point defect needs to be specified prior to solution. Thus, it is necessary to first examine how the defect parameters would vary with different core sizes. We calculate the Kanzaki force dipole tensor $\boldsymbol{M}$ and the formation energy V_f for different core sizes for the aforementioned point defects in the relaxed homogeneous Si and Ge lattices. These parameters characterize the defect. The nonlinear core plus two more outer shells of atoms define the (nominal) defect space, which in turn determines the required computational effort.

In the relaxed Si and Ge matrices, the Kanzaki force dipole tensor of a defect is found to be hydrostatic with diagonal components $M_{11}=M_{22}=M_{33}$ and off-diagonal components equal to zero. Figures 4 and 5 show the variation of the percentage differences in M_{11} and V_f with the core sizes. The percentage differences are defined relative to the corresponding value for the maximum nonlinear core size considered here, which is eight shells of atoms. We see from Figs. 4 and 5 that the solutions converge with increasing nonlinear core size (artificially assigned). The nonlinear effect is significant in the core of substituted C, but relatively insignificant in the cores of other point defects. It should be noted that when a Si or a Ge atom is replaced by a C atom with surrounding atoms held in place, the bonding state between C and neighboring Si or Ge atoms falls on the downside along the force-bonding length curve, where the tangent stiffness is negative. This leads to an unstable solution where the Newton-Raphson iterative method fails. In this case, it is necessary to manually move the surrounding Si/Ge atoms close enough to the C atom so that the bonding state is on the upside of the force-bonding length curve. Then, the solution as outlined before can lead to the fully relaxed configuration $\boldsymbol{X}_F$.

Having verified the convergence of the Kanzaki force dipole tensor and formation energy of the aforementioned point defects, we now examine the values of these parameters in the strained as well as relaxed homogeneous Si and Ge lattices. The strained Si and Ge correspond to their QW states with lattice constants given in the previous section. In our simulations, a nonlinear core up to the fifth shell from the point defect is used, which is sufficiently large for accurate evaluation as shown in Figs. 4 and 5. The supercell size for calculating the hybrid GF is $20\times20\times20$ unit cells. The difference in results compared to the case with the cell size of $10\times10\times10$ unit cells is within 1%. The results are presented in Tables III and IV.

We see from Tables III and IV that, when the lattices are strained, the Kanzaki force dipole tensor is no longer hydrostatic, as in the case of relaxed lattices. The diagonal components M_{11} $(=M_{22})$ and M_{33} become different, while the

TABLE IV. Kanzaki force dipole tensor and formation energy of point defects in the relaxed and strained Ge matrices. The strained case corresponds to the QW state.

	Vacancy		C substitution		Si substitution	
	Uns. mtrx.	Str. mtrx.	Uns. mtrx	Str. mtrx	Uns. mtrx	Str. mtrx
M_{11} (eV)	2.64	−2.54	−15.4	−18.4	−1.33	−1.54
M_{22} (eV)	2.64	−2.54	−15.4	−18.4	−1.33	−1.54
M_{33} (eV)	2.64	2.02	−15.4	−15.8	−1.33	−1.24
V_f (eV)	3.60	3.59	−2.29	−3.22	−0.748	−0.829

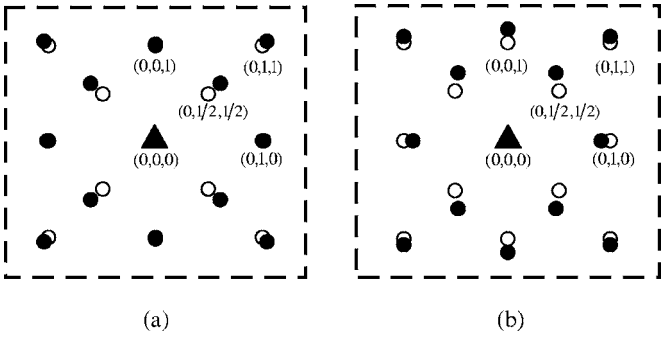

FIG. 6. Lattice distortion around a single vacancy in the relaxed (a) and strained (b) Ge matrices. The triangle indicates the vacancy. The open circles indicate the original (reference) atomic position. The solid circles indicate the final atomic position, with atomic displacement about the reference position magnified by 50 times. These atoms are in the same vertical plane of the vacancy.

off-diagonal components remain zero. The magnitudes of all these defect parameters change significantly when the lattices are strained as in their QW states. In particular, the sign of M_{11} $(=M_{22})$ is switched in the core of a single vacancy in the Ge lattice when it is strained from the bulk to the QW state. Figures 6(a) and 6(b) show the lattice distortion in a vertical plane containing a single vacancy at its center in the relaxed and the strained cases, respectively. In the case of the relaxed lattice, the atoms move outwards, that is, away from the vacancy. In contrast, when the lattice is strained as in the QW state, the atoms move laterally inwards but vertically outwards. This behavior indicates a buckling-type bifurcation phenomenon of deformation mode in the core of a single vacancy with the strain in the Ge lattice as the parameter. A more detailed study of this phenomenon is in progress.

As may be expected from Tables III and IV, the core structure of a point defect changes abruptly near a Si/Ge interface in Si-Ge QWs. The detailed variation of the Kanzaki force dipole tensor and formation energy with distance from the lower interface is shown for a vacancy and substitutional C in Si/Ge/Si and Ge/Si/Ge QWs in Figs. 7–10, respectively. The interface is located at zero depth, and the QW of either Si or Ge is on the positive side. Notice that the Kanzaki force dipole tensor shows a relatively smooth transition across the interface, with its diagonal components splitting when the defects move from the relaxed into the strained lattice. The component M_{12} $(=M_{21})$ becomes nonzero, although small near the interface. The other off-diagonal components remain equal to zero. The formation

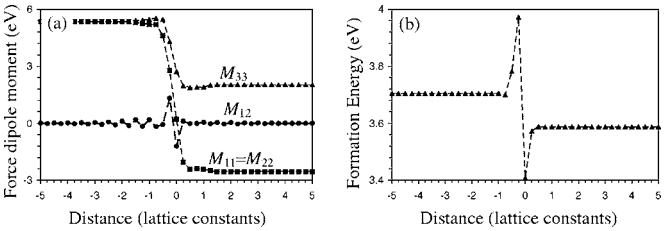

FIG. 7. Variation of (a) Kanzaki force dipole tensor and (b) formation energy of a vacancy with distance from an interface in the Si/Ge/Si QW.

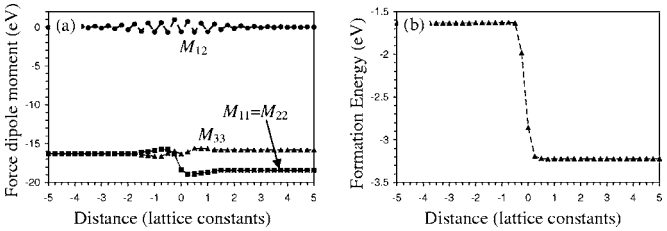

FIG. 8. Variation of (a) Kanzaki force dipole tensor and (b) formation energy of a C substitution with distance from an interface in the Si/Ge/Si QW.

energy of a substituted C makes a smooth transition in both the Si/Ge/Si and Ge/Si/Ge QWs. In contrast, the formation energy of a vacancy shows spikes and a large jump across the interface. From these figures, it is clear that the transition in the defect core structure extends over a distance ranging from two to four lattice constants, depending on the defect species. The plateaus in these figures are equal to the corresponding defect parameters in the bulk matrices, as given in Tables III and IV.

V. CONCLUSIONS

We have developed an efficient and accurate GF method to model point defects in Si-Ge QWs. The model includes nonlinear effects and accounts for the elastic anisotropy. The trilayer LSGF and CGF, which give the response to a point force in the reference solid at different length scales, are combined seamlessly to solve the multiscale problem of point and extended defects. The method is based on the Dyson equation, which relates the defect and the reference LSGF, and on the asymptotic approach of the reference LSGF to the reference CGF at large distances from the point force. Nonlinearity in the core region around a point defect is taken into account by using an iterative scheme.

The Tersoff potential[23] is used to model the heterogeneous system with point defects that include a vacancy and substitutional impurities. It is used to set up the reference lattice, calculate the force constants in the lattice, and derive the elastic constants of the bulk solids needed for calculating the CGF. The hybrid GF is defined as the reference LSGF which is obtained by solving the lattice-statics problem of a supercell of atoms subject to the CGF boundary condition. The hybrid GF converges well with the size of the supercell. The (converged) reference LSGF approaches the CGF at large

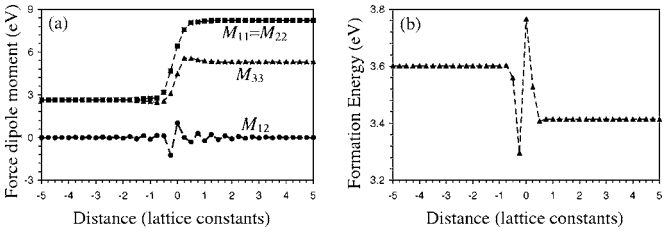

FIG. 9. Variation of (a) Kanzaki force dipole tensor and (b) formation energy of a vacancy with distance from an interface in the Ge/Si/Ge QW.

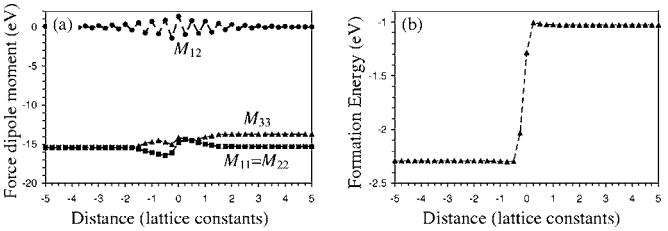

FIG. 10. Variation of (a) Kanzaki force dipole tensor and (b) formation energy of a C substitution with distance from an interface in the Ge/Si/Ge QW.

distances from the point force, but they are generally different in the vicinity of the point force. It is found that the differences are significant only within a fairly small distance. Hence the reference LSGF can be efficiently and accurately evaluated, which provides an efficient and accurate solution of the problem of multiscale modeling of point defects in Si-Ge QWs.

After the lattice distortion is obtained by the GF method, the Kanzaki force dipole tensor and formation energy of various point defects are calculated. These quantities are required for stress and defect-diffusion analyzes in a phenomenological formulation. The calculated formation energy of a single vacancy in relaxed bulk Si is consistent with that previously reported in the literature.[34] The formation energy and the Kanzaki force dipole tensor of various point defects in strained as well as relaxed bulk Si and Ge lattices are also calculated. It is found that these defect parameters are changed significantly by the straining in the QW states. In particular, there appears to be a buckling-type bifurcation of deformation mode in the core region of a single vacancy in Ge lattice, with the strain in the lattice as the parameter. These defect parameters are also examined in Si/Ge/Si and Ge/Si/Ge QWs, which gives detailed information about the core structure of the point defects near an abrupt Si/Ge interface. The transition of defect core structure across an interface normally extends to about two to four lattice constants, depending on the defect species. This study provides the input parameters required for a continuum modeling of point defects in the Si-Ge systems and also for a quantum mechanical calculation of the electron wave functions that requires the precise location of atoms near the defects. It is hoped that this work will form the basis for further study of point defects in nanostructure devices.

ACKNOWLEDGMENTS

The authors thank T. P. Quinn and D. T. Read for reading the manuscript and helpful suggestions.

*Correspondence author. Electronic address: boyang@fit.edu

[1] H. Kanzaki, Phys. Chem. Solids **2**, 24 (1957).
[2] J. A. Van Vechten, Phys. Rev. B **10**, 1482 (1974).
[3] A. G. Milnes, *Deep Impurities in Semiconductors* (John Wiley and Sons, New York, 1973).
[4] *Deep Centers in Semiconductors: A State-of-the-Art Approach*, edited by S. T. Pantelides (Gordon and Breach Science Publishers, New York, 1986).
[5] T. Mura, *Micromechanics of Defects in Solids* (Martinus Nijhoff Publishers, Boston, 1982).
[6] J. D. Eshelby, in *Solid State Physics: Advances in Research and Applications*, edited by F. Seitz and D. Turnbull (Academic Press, New York, 1956).
[7] A. J. Read, R. J. Needs, K. J. Nash, L. T. Canham, P. D. J. Calcott, and A. Qteish, Phys. Rev. Lett. **69**, 1232 (1992).
[8] H. Sawada and K. Kawakami, Phys. Rev. B **62**, 1851 (2000).
[9] M. Tang, L. Colombo, J. Zhu, and T. Diaz de la Rubia, Phys. Rev. B **55**, 14279 (1997).
[10] A. V. Krasheninnikov, K. Nordlund, M. Sirviö, E. Salonen, and J. Keinonen, Phys. Rev. B **63**, 245405 (2001).
[11] A. A. Maradudin, E. W. Montroll, G. H. Weiss, and I. P. Ipatova, *Theory of Lattice Dynamics in the Harmonic Approximation*, Solid State Physics Supp 3, 2nd edition, edited by H. Ehrenreich, F. Seitz, and D. Turnbull (Academic Press, New York; 1971).
[12] V. K. Tewary, Adv. Phys. **22**, 757 (1973).
[13] J. E. Sinclair, P. C. Gehlen, R. G. Hoagland, and J. P. Hirth, J. Appl. Phys. **49**, 3890 (1978).
[14] S. Rao, C. Hernandez, J. P. Simmons, T. A. Parthasarathy, and C. Woodward, Philos. Mag. A **77**, 231 (1997).
[15] V. K. Tewary, Phys. Rev. B **69**, 094109 (2004).
[16] B. Yang and V. K. Tewary, Int. J. Solids Struct. **42**, 4722 (2005).
[17] M. Lannoo and J. Bourgoin, *Point Defects in Semiconductors I*, Springer Series in Solid-State Sciences 22 (Springer Verlag, New York, 1981).
[18] J. Stangl, V. Holý, and G. Bauer, Rev. Mod. Phys. **76**, 725 (2004).
[19] P. Harrison, *Quantum Wells, Wires and Dots: Theoretical and Computational Physics* (John Wiley & Sons, New York, 2002).
[20] D. Bimberg, M. Grundmann, and N. Ledentsov, *Quantum Dot Heterostructures* (John Wiley, New York, 1999).
[21] M. A. Makeev and A. Madhukar, Phys. Rev. B **67**, 073201 (2003).
[22] J. G. Swadener, M. I. Baskes, and M. Nastasi, Phys. Rev. B **72**, 201202(R) (2005).
[23] J. Tersoff, Phys. Rev. B **39**, 5566 (1989).
[24] M. I. Baskes, Phys. Rev. B **46**, 2727 (1992).
[25] J. F. Justo, M. Z. Bazant, E. Kaxiras, V. V. Bulatov, and S. Yip, Phys. Rev. B **58**, 2539 (1998).
[26] R. Benedek and P. S. Ho, J. Phys. F: Met. Phys. **3**, 1285 (1973).
[27] R. Thomson, S. J. Zhou, A. E. Carlsson, and V. K. Tewary, Phys. Rev. B **46**, 10613 (1992).
[28] B. Yang and E. Pan, Eng. Anal. Boundary Elem. **26**, 355 (2002).
[29] B. Yang and E. Pan, Int. J. Solids Struct. **39**, 2235 (2002).
[30] V. K. Tewary, E. R. Fuller, and R. M. Thomson, J. Mater. Res. **4**, 320 (1989).
[31] J. N. Reddy, *An Introduction to Nonlinear Finite Element Analysis* (Oxford University Press, London, 2004).
[32] T. Belytschko, W. K. Liu, and B. Moran, *Nonlinear Finite Elements for Continua and Structures* (John Wiley & Sons, New

York, 2000).
[33] J. Cormier, J. M. Rickman, and T. J. Delph, J. Appl. Phys. **89**, 99 (2001).
[34] H. Balamane, T. Halicioglu, and W. A. Tiller, Phys. Rev. B **46**, 2250 (1992).
[35] T. C. T. Ting, *Anisotropic Elasticity* (Oxford University Press, London, 1996).
[36] P. N. Keating, Phys. Rev. **149**, 674 (1966).
[37] M. Born and K. Huang, *Dynamical Theory of Crystal Lattices* (Oxford University Press, London, 1998).